Since January 2020 Elsevier has created a COVID-19 resource centre with free information in English and Mandarin on the novel coronavirus COVID-19. The COVID-19 resource centre is hosted on Elsevier Connect, the company's public news and information website.

32

A novel machine learning–based detection and diagnosis model for coronavirus disease (COVID-19) using discrete wavelet transform with rough neural network

Irina Valeryevna Pustokhina[1], Denis Alexandrovich Pustokhin[2], K. Shankar[3]

[1]PLEKHANOV RUSSIAN UNIVERSITY OF ECONOMICS, MOSCOW, RUSSIAN FEDERATION; [2]STATE UNIVERSITY OF MANAGEMENT, MOSCOW, RUSSIAN FEDERATION; [3]DEPARTMENT OF COMPUTER APPLICATIONS, ALAGAPPA UNIVERSITY, KARAIKUDI, TAMIL NADU, INDIA

1. Introduction

Coronavirus (CoV) disease-2019 (COVID-19) a pandemic that emerged in Wuhan, China and evolved as a danger to health all over the world [1–5]. CoVs are a massive group of viruses including Middle East respiratory syndrome (MERS-CoV) and severe acute respiratory syndrome (SARS-CoV). COVID-19 is a new type found in 2019 that was discovered in humans. CoVs are zoonotic because of the contamination of animals to humans. COVID-19 is transferred from bats to humans. When COVID-19 causes minor symptoms, it sometimes becomes critical [6–8]. There have been around 335,403 CoV cases; among them, 14,611 died and 97,636 recovered. There were about 223,156 infected patients. Many of the people are affected by COVID-19 and it leads to an increase in death rate. The symptoms of virus infection are respiratory problems, a cold, a sore throat, a high fever, and shortness of breath. In the critical condition, it leads to pneumonia, SARS, septic shock, and multiple-organ failures, and then death [9,10]. It is estimated that men are more affected than women; fortunately, no children are affected by COVID-19. The respiratory value of patients with COVID-19 pneumonia has been depicted to show better results [11–14]. In many developed countries, health systems

Data Science for COVID-19. https://doi.org/10.1016/B978-0-12-824536-1.00009-5

have become complex one because they have suddenly needed upgraded intensive care units, which have filled with COVID-19 patients. The transmission of COVID-19 has globally increased in a short span of time.

Based on guidelines issued by China, the analysis of COVID-19 has to be verified by gene sequences as a major sign for reverse transcription polymerase chain reaction (RT-PCR). Moreover, the COVID-19 is found to be infectious and it can be easily spread over the people [15]. Infected patients are screened using computed tomography (CT), which shows opacities to be denser and more profuse, and confluent compared with the images of normal lungs. This invention helps diagnose pneumonia. A search for excess nucleic acids with the help of multiple PCR of well-known pathogen panels can generate a negative outcome and a diagnosis of pneumonia [16–20]. Some samples from patients' bronchoalveolar lavage fluid are used to analyze pathogens that have a genetic sequence identical to β-coronavirus B lineage. The newly found samples comprises of ~80%, ~50%, and ~96%, which identifies the genome of SARS-CoV, MERS-CoV, bat CoV, and RaTG13, correspondingly. The new CoV was termed SARS-CoV-2, the pathogen causing COVID-19. The disease was transmitted in at least 202 countries; one million people were affected, resulting in a massive death rate globally [21]. In addition, it is thought that COVID-19 infections were miscalculated, because there were more asymptomatic cases, which were not predicted. Based on the *Diamond Princess* cruise ship case literature, there were several unpredicted cases. These patients are highly infectious and able to spread the disease to other persons [22].

SARS-CoV-2 is a communicable disease among humans. A study revealed that the initial transmission of the disease take place through bats [23–25]. It is also calculated that a person affected by SARS-CoV-2 affected would spread the disease to least three to four people. The symptoms may differ among people, and many remain untreated, whereas others will have a high fever, cold, dyspnea, and many other signs. The disease may be transmitted by direct contact and physical touch. The current hypothesis states that the aerosol and surface reliability of SARS-CoV-2 showcases that the virus might be identified in aerosols (<5 μm) and it is reliable for plastic and stainless steel compared with copper and cardboard.

The traditional models imply that the maximum number of patients are affected with COVID-19. Such patients have medical symptoms such as fever and a cold. Imaging is a significant diagnostic tool for estimating the infection. The consequent diagnosis depends on real-time RT-PCR positivity for the existence of CoV. Because of the robust infection of COVID-19, robust and exact diagnosing techniques are essential for finding, isolating, and treating patients immediately, to decrease the lethal effects and the threat of public transmission. Therefore, RT-PCR requires a long time whereas CT results can be attained rapidly.

The US Food and Drug Administration has accepted medicines for treating COVID-19 patients. Diagnostics has a significant role slowing in the transmission of COVID-19. It enables the fast execution of metrics that reduce the spread over case investigations,

isolation, and contact observations. The signs of COVID-19 patients are nonspecific, which does not help in diagnosing the disease. Furthermore, studies reveal that the affected patients have a cough, fatigue, sputum, and difficulty breathing. Nucleic acid testing and CT scans are applied to diagnose and predict COVID-19. Molecular methods are highly applicable compared with syndrome testing, and CT scans are helpful in an accurate analysis to find particular pathogens. The establishment of molecular methods is based on the proteomic as well as genomic composition of a pathogen. The composition of SARS-CoV-2 was found, but an examination of the virus is still a black box.

A primary genome sequence of SARS-CoV-2 was carried out with metagenomic RNA sequencing and unbiased as well as maximum throughput used in various genomes. These findings were enclosed and included in a GenBank sequence repository. Followed by, Global Initiative on Sharing All Influenza Data and GenBank provides massive amount of data from all over the world [26]. Based on the report provided by the World Health Organization (WHO), 104 strains of the SARS-CoV-2 virus were separated and sequenced under the application of Illumina and Oxford nanopore sequencing. Illumina sequencing is defined as the sequence-by-synthesis model with the help of applying solid-phase bridge amplification, whereas nanopore sequencing contributes the translocation of a DNA molecule using a protein pore and calculating the consequent shifts in voltage to compute the DNA sequence. Based on WHO reports, the adverse priority for COVID-19 diagnosing research offers nucleic acid as well as protein tests to predict the point-of-care (PoC). The higher priority is to combine the tests into several blocks. To enhance surveillance measures, serological tests with proteins are required. The PoC is more expensive, hand-based tools applied to examine the patients. It is operated in regions such as community centers, which results in reducing the overhead of medical laboratories. The accessibility of deployed diagnostic models has activated the plug-and-play approach in diagnosing the COVID-19 pandemic. These models alleviate enhancement, but it is vital to find more about COVID-19 and prevent the disease from spreading.

On the other hand, laboratory reports on the virus show that artificial intelligence (AI)-based models are capable of the initial prediction of a virus, and alert people to prevent disease transmission. The virus sequence from such detection tools was extended to help developers all over the world to discover medicine and enhance the diagnostic process. The virus is mapped in an open database in which laboratories are accredited by the WHO to improve investigations for vaccinations. Also, some of the infected people does not have any symptoms and it results in rapid spreading of diseases [27]. Many developers are capable of dividing and treating patients immediately. Even if COVID-19 does not result in death, unrecoverable lung infection may be outcome.

Based on the WHO, COVID-19 tends to open holes in lungs as in SARS, by causing a "honeycomb-like structure" [28]. CT is a scanning system used to screen brain disease, pneumonia, and so on. AI relies on automatic CT image prediction devices for the

detecting, quantification, and observation of CoV and differentiates patients affected with CoV, as shown in Gozes et al. [29]. Butt et al. [30] focused on developing a primary screening method to differentiate COVID-19 pneumonia as well as influenza A viral pneumonia from normal cases by applying lung CT images and deep learning (DL) methods.

Shuai et al. [31] proposed an approach based on COVID-19 modifications from CT images, which was deployed with DL and extracts graphical features of COVID-19 to offer a medical diagnosis; it saves time in analyzing the disease. MERS-CoV and SARS-CoV are said to be similar to COVID-19. The work of Ahmet Hamimi implied that some features shown on chest X-ray and CT demonstrate the manifestation of pneumonia [32]. The study of Xuanyang et al. [33] presented data mining methods employed to differentiate SARS from general pneumonia according to X-ray images. CT scans are an extended version of X-ray tools. They determine normal and abnormal soft structures. The application of X-rays is robust, simple, cheap, and less harmful compared with CT. The primary detection of disease tends to improve the lifetime of an individual.

This chapter introduces a feature extraction-based classification model using discrete wavelet transform (DWT) with a rough neural network (RNN). Principal component analysis (PCA) also takes place to reduce the subset of features before classification. For experimental analysis, the DWT-RNN models undergo validation against a chest X-ray dataset.

2. The proposed discrete wavelet transform—rough neural network model

The overall process diagram of the DWT-RNN model is depicted in Fig. 32.1, which details its working process. At the first level, preprocessing takes place to improvise the image quality. Then, the preprocessed images undergo feature extraction in which useful features are extracted from the image using DWT. Then, feature reduction is carried out, and finally, classification takes place with the RNN model.

2.1 Discrete wavelet transform—based feature extraction

The traditional signal analysis is Fourier transform (FT), which falls below the time domain signal into constituent sinusoids of diverse frequencies, which converts the signal from time domain to frequency domain. Therefore, FT is composed with the critical limitation of leaving out the time details of a process. Hence, the classification task might be removed owing to the loss of time details. Gabor applied the FT to examine a signal simultaneously. This model is named short-time FT (STFT). It includes a window that should be definite structure. STFT refers to a settlement among time and frequency details. Therefore, the precision of data has been minimized by the window size. Wavelet transform (WT) implies that a windowing model is composed with a

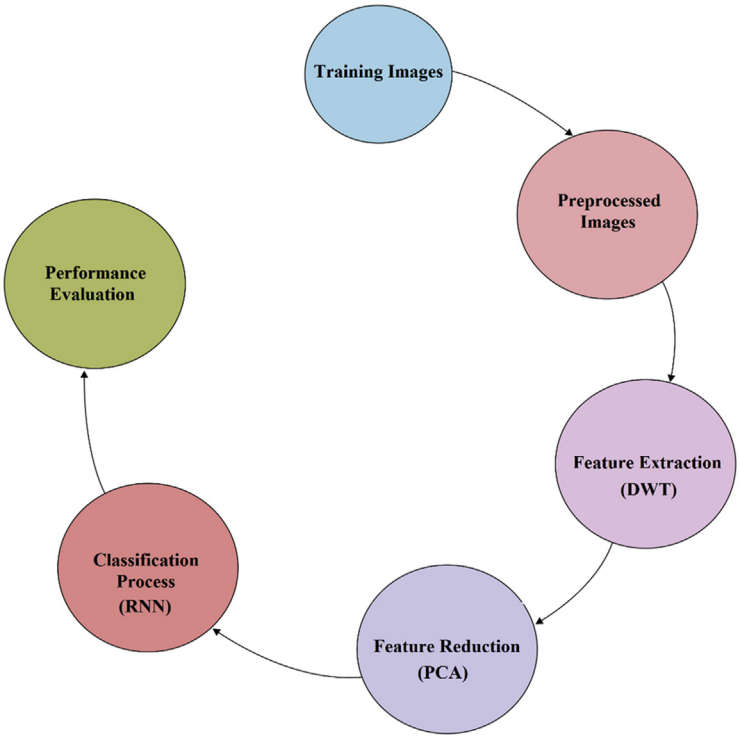

FIGURE 32.1 Working process of proposed method. *DWT*, discrete wavelet transform; *PCR*, polymerase chain reaction; *RNN*, rough neural network.

variable size. Hence, it conserves the time and frequency data of a signal. The additional merit of WT is that it applies a scale rather than a conventional frequency, which cannot generate a time frequency and produce the time-scale view. It is said to be diverse way to observe data, but it effective.

2.1.1 Discrete wavelet transform

The DWT is said to be an efficient execution of WT with the application of dyadic scales and positions. When $x(z)$ implies a square-integrable function, a continuous WT of $x(z)$ related to the provided $\psi(z)$ is represented as:

$$W_{\psi}(a,b) = \int_{-\infty}^{\infty} x(t)\psi_{a,b}(z)dz, \tag{32.1}$$

where:

$$\psi_{a,b}(z) = \frac{1}{\sqrt{a}}\psi\left(\frac{t-a}{b}\right). \tag{32.2}$$

Wavelet $\psi_{ab}(z)$ has been computed from the mother wavelet $\psi(z)$ by translation as well as dilation. Here, a is named the dilation factor, and b is a translation parameter.

It has various types of wavelets that gained popularity from the growth of WT. The vital objective is the Harr wavelet, which is simple and is preferred by every domain.

Eq. (32.1) could be discretized by refining a and b to a discrete lattice $(a = 2^b \& a > 0)$as an applied DWT represented as:

$$ca_{u,v}(n) = DS\left[\sum_n x(n) g_u^*(n - 2^u v)\right], \tag{32.3}$$

$$cd_{u,v}(n) = DS\left[\sum_n x(n) h_u^*(n - 2^u v)\right]. \tag{32.4}$$

In this approach, $ca_{u,v}$ and $cd_{u,v}$ denote a coefficients of approximation units and brief units, respectively. $g(n)$ and $h(n)$ show a low-pass filter and high-pass filter, respectively. u and v denotes the wavelet scale and translation aspects, and the DS operator is named down-sampling. The predefined decomposition process could be processed with preceding approximations degraded in the future; thus, a signal is broken down into diverse resolution levels. The complete process is named a wavelet decomposition tree.

2.1.2 Two-dimensional discrete wavelet transform

For two-dimensional (2D) 2Dimages, the DWT has been used for every dimension. The schematic architecture of 2Dof 2D DWT is depicted in Fig. 32.3. Finally, it has four subbands, such as low-low (LL), low-high (LH), high-high (HH), and high-low (HL) images for every scale. Subband LL is applied for 2D DWT, as shown in Fig. 32.2. The LL subband is named the approximation unit, whereas the LH, HL, and HH subbands are termed brief components of an image. Because the decomposition level has been improved, a more compact and coarse approximation element is attained. Hence, the wavelet offers an elegant hierarchical approach to interpret the image data. Here, leve1 3 decomposition through the Harr wavelet performs the feature extraction task.

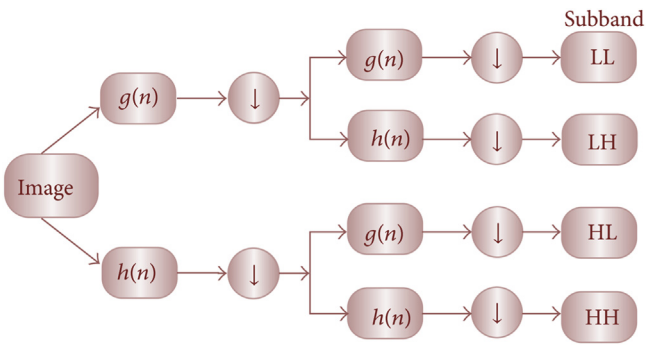

FIGURE 32.2 Representation of two-dimensional discrete wavelet transform.

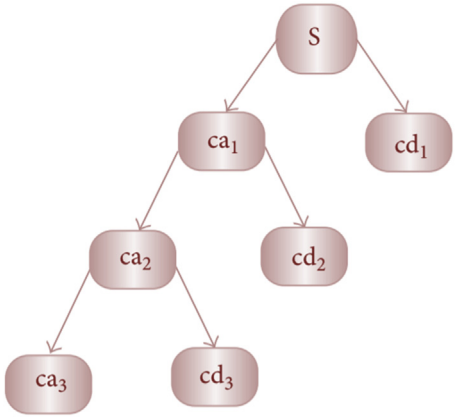

FIGURE 32.3 Three-level wavelet decomposition tree.

2.2 Polymerase chain reaction–based feature reduction

Additional features improve the processing time and memory space. Moreover, classification becomes tedious; that is the curse of dimensionality. There is a need to minimize the feature values. PCA is said to be an effective device to decrease the data dimension for a group of interlinked variables when maintaining the maximum difference. These models are composed with three objectives: they orthogonalize the elements of input vectors, and hence can be released from one another; they order the final orthogonal elements; and the maximum variation is arrived at initially, which avoids the minimum variations of a dataset. The input vectors must be normalized to have zero mean and unity variance before PCA is performed. Normalization is said to be a benchmark strategy. Data regarding a PCA can be acquired.

2.3 Rough neural network–based classification

Rough set and neural network (NN) methods are capable of resolving difficult as well as high-dimensional issues; they are called RNNs. A rough neuron could be obtained in the form of neuron pairs, in which a single neuron corresponds to the upper boundary and the alternate corresponds to the lower boundary. Rough set theory is a tool employed to predict uncertain data, and inference decision-making is carried out under the application of information systems. Fig. 32.4 depicts the model of RNN classifier.

$BND_P(Q)$ values are assumed to be uncertain measures, and inference decision-making has been processed under the application of similarity value (Eq. 32.5).

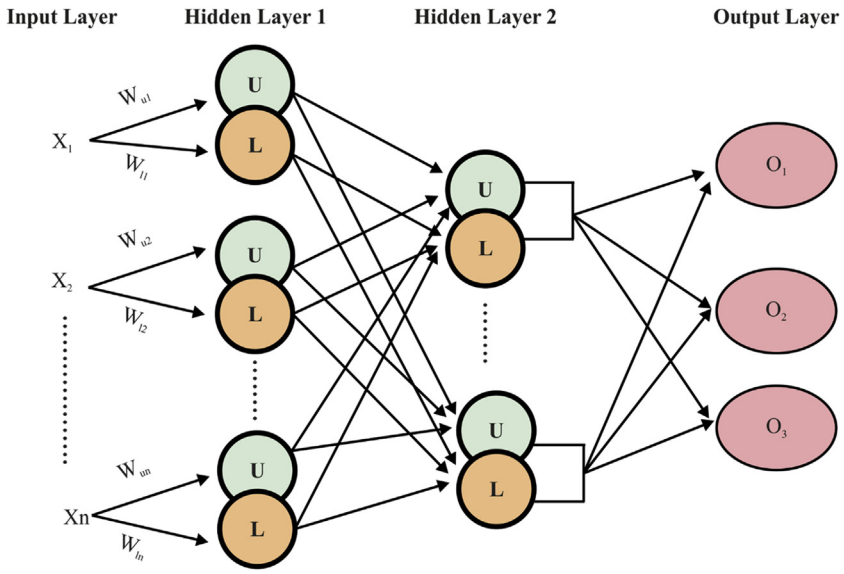

FIGURE 32.4 Architecture of rough neural network.

The similarity value is estimated for every element of $\mathrm{BND_P(Q)}$ using a centroid of all classes with minimum approximation $x \in \bigcup U / \underline{Q}^{PX(D)}$, and a decision value would be upgraded on the basis of a nearby centroid:

$$D_{uv} = \sum_{k=1}^{n} \sqrt{(X_{uk} - X_{vk})^2} \tag{32.5}$$

The classical neuron becomes replaced by an RNN model with a pair of neurons (lower and upper neurons) to represent the approximation of all attributes present in the dataset. It has a set of four inputs, two hidden and output layers. The hidden layers are composed of rough neurons that overlap and exchange details among one another. Processes involved in the RNN-based classification are listed next. The RNN operates on three major levels: preprocessing, training, and testing.

2.3.1 Level 1: preprocessing

1. Read all features that exist in every object of the database
2. Normalization of the values in the data takes place using the Eq. (32.6):

$$Norm = \frac{X - \min}{\max - \min} \tag{32.6}$$

2.3.2 Level 2: training

3. Initialization of arbitrary (upper, lower) weights of the network

4. Feed forward of feature values and perform multiplication in all directions (U_w, L_w)

5. Determine (I_U, I_L) of hidden layers using:

$$I_{Ln} = \sum_{J=1}^{n} W_{Lnj} O_{nj} \tag{32.7}$$

$$I_{Un} = \sum_{J=1}^{n} W_{Unj} O_{nj} \tag{32.8}$$

6. Determine (O_U, O_L) of hidden layers using:

$$O_{Ln} = Min(f(I_{Ln}), f(I_{Un})) \tag{32.9}$$

$$O_{Un} = Max(f(I_{Ln}), f(I_{Un})) \tag{32.10}$$

7. Ensure the diagnosis based on the original output (T) and output value (O), as defined in Eq. (32.11):

$$O = O_{Ln} + O_{Un} \tag{32.11}$$

8. When the outcome is an error, use the backpropagation algorithm and determine the error:

$$\Delta = T - O \tag{32.12}$$

9. Update (upper, lower) the weights of the network by deriving the activation function: new weight = old weight + (Δ *η *derivative* activation of (input)) where η is learning rate of model

10. Iterate the process from steps 6–8 until the reduced error is attained.

2.3.3 Level 3: testing phase

11. Classification of fresh samples takes place; compute the accuracy.

3. Performance validation

3.1 Dataset description

The experimental analysis of the proposed model takes place using a COVID chest X-ray dataset [34]. It is composed of a set of 60 images and 15 images under the classes of acute respiratory distress syndrome, COVID, SARS, and normal. Fig. 32.5 shows the sample set of test images.

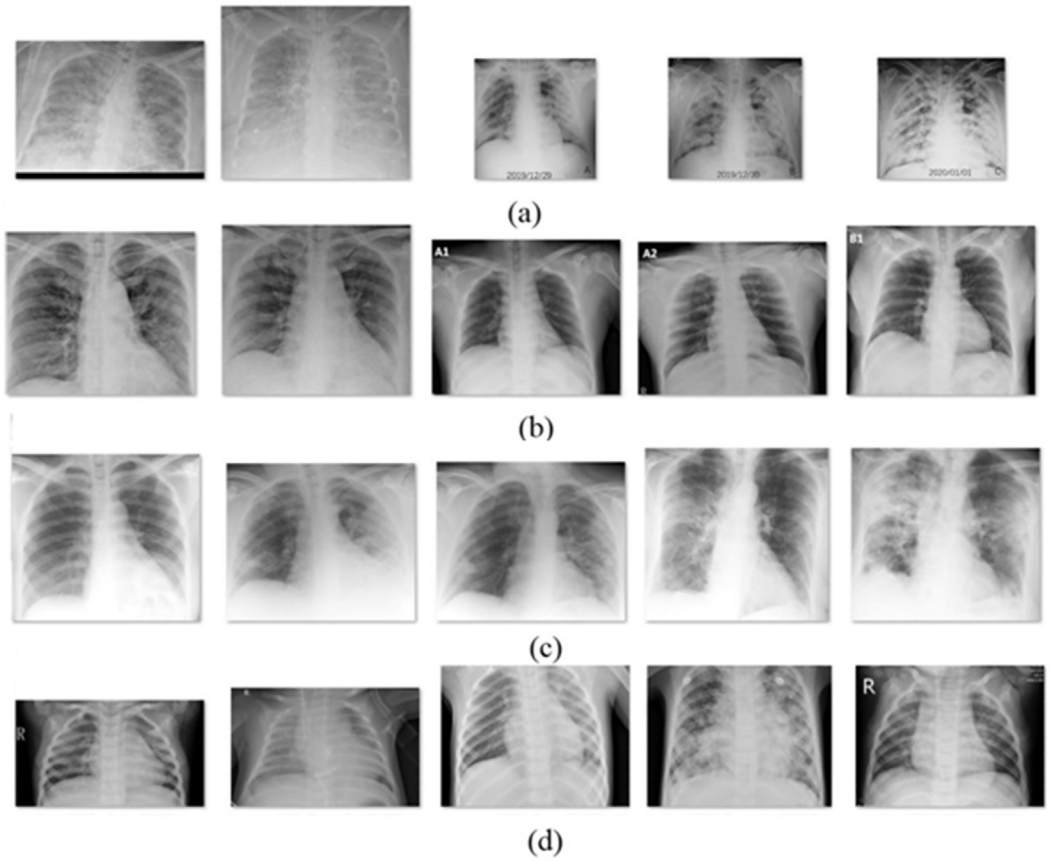

FIGURE 32.5 (A) Acute respiratory distress syndrome; (B) coronavirus disease-2019 images; (C) severe acute respiratory syndrome; (D) normal images.

3.2 Results of analysis

Fig. 32.6 shows the visualization of the original image and the preprocessed image in which artifacts present in the image are discarded. This figure exhibited the effective results of the applied model on the test input image.

Table 32.1 demonstrates the comparative analysis of the projected and existing models. Fig. 32.7 shows the comparative analysis in terms of sensitivity. The DWT model required a minimum sensitivity of 65.30% whereas the NN models reached a slightly higher sensitivity of 67.04%. In the same way, the GBT model achieved a better outcome of sensitivity value of 72.19%. However, the proposed DWT-RNN model had an effective outcome and achieved a maximum sensitivity of 78.39%.

Fig. 32.8 defines the comparative analysis with respect to specificity. The DWT model required a minimum specificity of 69.52% whereas the NN models reached a slightly

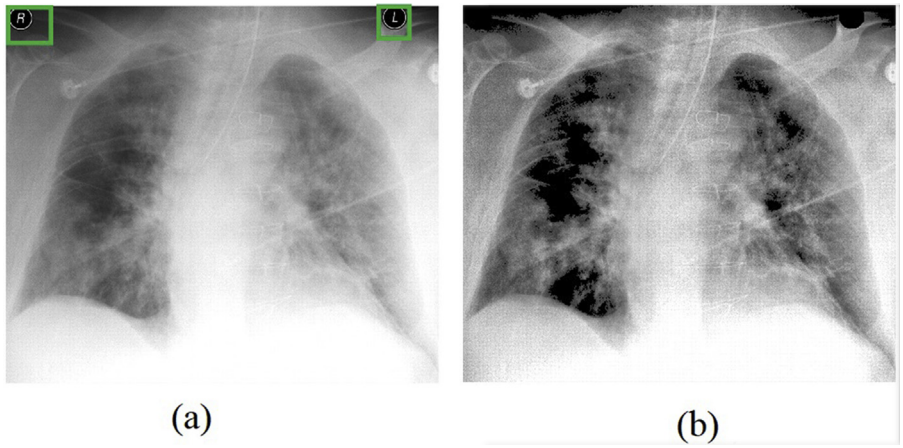

FIGURE 32.6 (A) Original image; (B) Image with artifacts removed.

Table 32.1 Classifier results analysis of discrete wavelet transform–rough neural network with existing models.

Methods	Sensitivity	Specificity	Accuracy	Kappa
Discrete wavelet transform– rough neural network	78.39	81.03	80.26	79.59
Neural network	67.04	71.74	70.37	70.22
Gradient boosting tree (GBT) [35]	72.19	75.88	73.96	72.85
Decision tree	65.30	69.52	66.84	66.30

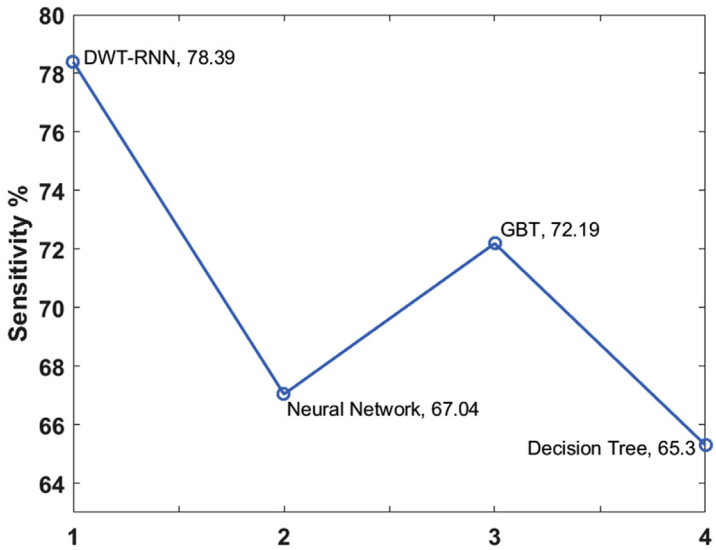

FIGURE 32.7 Sensitivity analysis of existing models. *DWT-RNN*: discrete wavelet transform– rough neural network; *GBT*: gradient boosting tree.

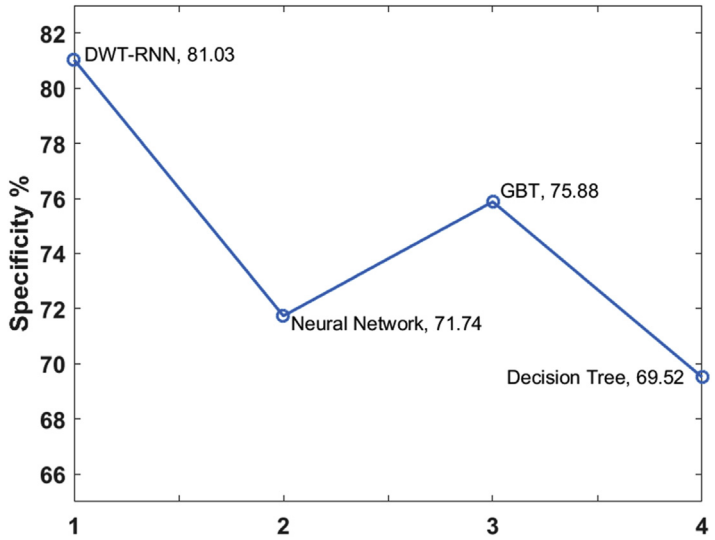

FIGURE 32.8 Specificity analysis of existing models. *DWT-RNN*: discrete wavelet transform– rough neural network; *GBT*: gradient boosting tree.

higher specificity of 71.74%. Moreover, the GBT model achieved a better outcome of specificity value of 75.88%. However, the proposed DWT-RNN model had achieved an optimal specificity of 81.03%.

Fig. 32.9 demonstrates the comparative analysis with respect to accuracy. The DWT model required a lower accuracy of 66.84% whereas the NN models had a moderate

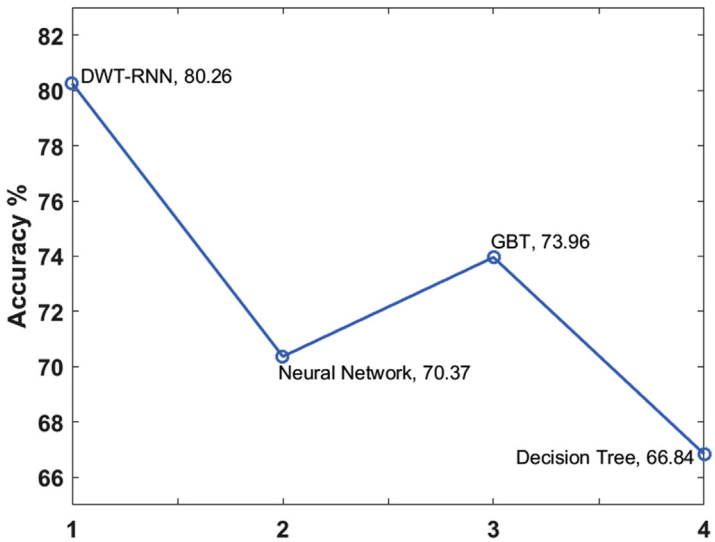

FIGURE 32.9 Accuracy analysis of existing models. *DWT-RNN*: discrete wavelet transform– rough neural network; *GBT*: gradient boosting tree.

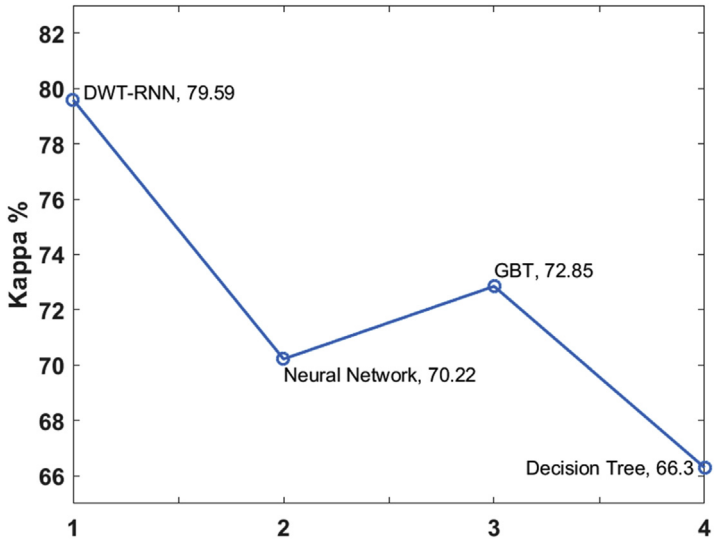

FIGURE 32.10 Kappa analysis of existing models. *DWT-RNN*: discrete wavelet transform– rough neural network; *GBT*: gradient boosting tree.

accuracy of 70.37%. In line with this, the GBT model reached a better accuracy of 73.96%. Hence, the proposed DWT-RNN model had optimal outcomes with a greater accuracy of 80.26%.

Fig. 32.10 depicts the comparative analysis by means of kappa. The DT model needed a lower kappa of 66.30% whereas the NN models attained a slightly better kappa value of 70.22%. Likewise, the GBT model reached a better kappa value of 72.85%. Therefore, the DWT-RNN model had efficient outcomes with a higher kappa of 79.59%. From these figures and tables, it is evident that the DWT-RNN model performed well compared with previous methods for an effective identification of COVID-19. Hence, it was successfully applied as a proper diagnostic tool in actual hospitals.

After an examination of the performance of the proposed model on the applied dataset, it is evident that the model is superior to other methods for several aspects. It had a sensitivity of 78.39%, specificity of 81.03%, accuracy of 80.26%, and kappa value of 79.59%. Hence, it was successfully applied as a proper diagnostic tool in actual hospitals.

4. Conclusion

COVID-19 was primarily identified in Hubei Province, China. A group of patients were admitted with colds, fevers, difficulty breathing, and many other symptoms. The signs represented by COVID-19 patients are nonspecific, which does not help in diagnosing the disease accurately. Advances in AI models are essential for regularizing and speeding the diagnosis of COVID-19 patients. To satisfy the existing needs for COVID-19

diagnoses, it is critical to develop an automated diagnostic model to identify the disease accurately and more quickly. This research has developed a new machine learning–based diagnostic model using DWT-RNN. At the first level, preprocessing takes place to improvise the image quality. Then, preprocessed images undergo feature extraction using DWT, in which useful features are extracted from the image using DWT. Then, feature reduction is carried out, and finally, classification process takes place by the RNN model. The DWT-RNN model was validated using a COVID chest X-ray dataset. The experimental outcome was validated for several aspects and the obtained results showed that the DWT-RNN model offers the best classification performance and saves time in controlling diseases. The simulation outcome ensured that the DWT-RNN model offers the best results with the highest sensitivity of 78.39%, specificity of 81.03%, accuracy of 80.26%, and kappa value of 79.59%.

Acknowledgment

Dr. K. Shankar sincerely acknowledges the financial support of the RUSA–Phase 2.0 Grant sanctioned vide Letter No. F. 24–51/2014-U, Policy (TNMulti-Gen), Dept. of Edn. Govt. of India, Dt. October 9, 2018.

References

[1] K. Roosa, Y. Lee, R. Luo, A. Kirpich, R. Rothenberg, J.M. Hyman, P. Yan, G. Chowell, Real-time forecasts of the COVID-19 epidemic in China from February 5th to February 24th, 2020, Infect. Dis. Modell. 5 (January 1, 2020) 256–263.

[2] www.nationalgeographic.com/science/2020/02/here-is-what-coronavirus-does-tothe-body/20.03.2020.

[3] Mahase E. Coronavirus: Covid-19 Has Killed More People than SARS and MERS Combined, Despite Lower Case Fatality Rate.

[4] Y. Wang, M. Hu, Q. Li, X.P. Zhang, G. Zhai, N. Yao, Abnormal Respiratory Patterns Classifier May Contribute to Large-Scale Screening of People Infected with COVID-19 in an Accurate and Unobtrusive Manner. arXiv Preprint arXiv:2002.05534, February 12, 2020.

[5] T. Ai, Z. Yang, H. Hou, C. Zhan, C. Chen, W. Lv, Q. Tao, Z. Sun, L. Xia, Correlation of chest CT and RT-PCR testing in coronavirus disease 2019 (COVID-19) in China: a report of 1014 cases, Radiology (February 26, 2020) 200642.

[6] Y. Li, L. Xia, Coronavirus disease 2019 (COVID-19): role of chest CT in diagnosis and management, Am. J. Roentgenol. (March 4, 2020) 1–7.

[7] L. Guo, L. Ren, S. Yang, M. Xiao, D. Chang, F. Yang, C.S. Dela Cruz, Y. Wang, C. Wu, Y. Xiao, L. Zhang, Profiling early humoral response to diagnose novel coronavirus disease (COVID-19), Clin. Infect. Dis. (March 21, 2020).

[8] S.P. Adhikari, S. Meng, Y.J. Wu, Y.P. Mao, R.X. Ye, Q.Z. Wang, C. Sun, S. Sylvia, S. Rozelle, H. Raat, H. Zhou, Epidemiology, causes, clinical manifestation and diagnosis, prevention and control of coronavirus disease (COVID-19) during the early outbreak period: a scoping review, Infect. Dis. Poverty 9 (1) (December 2020) 1–2.

[9] W. Han, B. Quan, Y. Guo, J. Zhang, Y. Lu, G. Feng, Q. Wu, F. Fang, L. Cheng, N. Jiao, X. Li, The course of clinical diagnosis and treatment of a case infected with coronavirus disease 2019, J. Med. Virol. 92 (5) (May 2020) 461–463.

[10] C. Long, H. Xu, Q. Shen, X. Zhang, B. Fan, C. Wang, B. Zeng, Z. Li, X. Li, H. Li, Diagnosis of the coronavirus disease (COVID-19): rRT-PCR or CT? Eur. J. Radiol. (March 25, 2020) 108961.

[11] W.J. Guan, Z.Y. Ni, Y. Hu, W.H. Liang, C.Q. Ou, J.X. He, L. Liu, H. Shan, C.L. Lei, D.S. Hui, B. Du, Clinical characteristics of coronavirus disease 2019 in China, N. Engl. J. Med. 382 (18) (April 30, 2020) 1708–1720.

[12] D.K. Chu, Y. Pan, S.M. Cheng, K.P. Hui, P. Krishnan, Y. Liu, D.Y. Ng, C.K. Wan, P. Yang, Q. Wang, M. Peiris, Molecular diagnosis of a novel coronavirus (2019-nCoV) causing an outbreak of pneumonia, Clin. Chem. 66 (4) (April 1, 2020) 549–555.

[13] S. Salehi, A. Abedi, S. Balakrishnan, A. Gholamrezanezhad, Coronavirus disease 2019 (COVID-19): a systematic review of imaging findings in 919 patients, Am. J. Roentgenol. (March 14, 2020) 1–7.

[14] M.J. Loeffelholz, Y.W. Tang, Laboratory diagnosis of emerging human coronavirus infections–the state of the art, Emerg. Microb. Infect. 9 (1) (January 1, 2020) 747–756.

[15] L.L. Poon, O.K. Wong, W. Luk, K.Y. Yuen, J.S. Peiris, Y. Guan, Rapid diagnosis of a coronavirus associated with severe acute respiratory syndrome (SARS), Clin. Chem. 49 (6) (June 1, 2003) 953–955.

[16] Y.H. Jin, L. Cai, Z.S. Cheng, H. Cheng, T. Deng, Y.P. Fan, C. Fang, D. Huang, L.Q. Huang, Q. Huang, Y. Han, A rapid advice guideline for the diagnosis and treatment of 2019 novel coronavirus (2019-nCoV) infected pneumonia (standard version), Mil. Med. Res. 7 (1) (December 1, 2020) 4.

[17] F. He, Y. Deng, W. Li, Coronavirus disease 2019: what we know? J. Med. Virol. (March 28, 2020).

[18] J.M. Sharfstein, S.J. Becker, M.M. Mello, Diagnostic testing for the novel coronavirus, JAMA 323 (15) (April 21, 2020) 1437–1438.

[19] R. Han, L. Huang, H. Jiang, J. Dong, H. Peng, D. Zhang, Early clinical and CT manifestations of coronavirus disease 2019 (COVID-19) pneumonia, Am. J. Roentgenol. (March 17, 2020) 1–6.

[20] Z.M. Chen, J.F. Fu, Q. Shu, Y.H. Chen, C.Z. Hua, F.B. Li, R. Lin, L.F. Tang, T.L. Wang, W. Wang, Y.S. Wang, Diagnosis and treatment recommendations for pediatric respiratory infection caused by the 2019 novel coronavirus, World J. Pediatr. (February 5, 2020) 1–7.

[21] M.J. Binnicker, Emergence of a novel coronavirus disease (covid-19) and the importance of diagnostic testing: why partnership between clinical laboratories, public health agencies, and industry is essential to control the outbreak, Clin. Chem. 66 (5) (May 1, 2020) 664–666.

[22] Z. Ye, Y. Zhang, Y. Wang, Z. Huang, B. Song, Chest CT manifestations of new coronavirus disease 2019 (COVID-19): a pictorial review, Eur. Radiol. (March 19, 2020) 1–9.

[23] A. Narin, C. Kaya, Z. Pamuk, Automatic Detection of Coronavirus Disease (Covid-19) Using X-Ray Images and Deep Convolutional Neural Networks. arXiv Preprint arXiv:2003.10849, March 24, 2020.

[24] M. Hosseiny, S. Kooraki, A. Gholamrezanezhad, S. Reddy, L. Myers, Radiology perspective of coronavirus disease 2019 (COVID-19): lessons from severe acute respiratory syndrome and Middle East respiratory syndrome, Am. J. Roentgenol. 214 (5) (May 2020) 1078–1082.

[25] E. Poggiali, A. Dacrema, D. Bastoni, V. Tinelli, E. Demichele, P. Mateo Ramos, T. Marcianò, M. Silva, A. Vercelli, A. Magnacavallo, Can lung US help critical care clinicians in the early diagnosis of novel coronavirus (COVID-19) pneumonia? Radiology (March 13, 2020) 200847.

[26] Y. Song, S. Zheng, L. Li, X. Zhang, X. Zhang, Z. Huang, J. Chen, H. Zhao, Y. Jie, R. Wang, Y. Chong, Deep learning enables accurate diagnosis of novel coronavirus (COVID-19) with CT images, medRxiv (January 1, 2020).

[27] P.K. Sethy, S.K. Behera, Detection of coronavirus disease (covid-19) based on deep features, Preprints (March 19, 2020) 2020030300, 2020.

[28] W. Zhang, Imaging changes of severe COVID-19 pneumonia in advanced stage, Intens. Care Med. (March 2, 2020) 1–3.

[29] O. Gozes, M. Frid-Adar, H. Greenspan, P.D. Browning, H. Zhang, W. Ji, A. Bernheim, E. Siegel, Rapid Ai Development Cycle for the Coronavirus (Covid-19) Pandemic: Initial Results for Automated Detection & Patient Monitoring Using Deep Learning Ct Image Analysis. arXiv Preprint arXiv:2003. 05037, March 10, 2020.

[30] C. Butt, J. Gill, D. Chun, B.A. Babu, Deep learning system to screen coronavirus disease 2019 pneumonia, Appl. Intell. (April 22, 2020) 1.

[31] S. Wang, B. Kang, J. Ma, X. Zeng, M. Xiao, J. Guo, M. Cai, J. Yang, Y. Li, X. Meng, B. Xu, A deep learning algorithm using CT images to screen for corona virus disease (COVID-19), MedRxiv (January 1, 2020).

[32] H.A. MERS-CoV, Middle East respiratory syndrome corona virus: can radiology be of help? Initial single center experience, Egypt. J. Radiol. Nucl. Med. 47 (1) (March 1, 2016) 95−106.

[33] G.J. Williams, S.J. Simoff (Eds.), Data Mining: Theory, Methodology, Techniques, and Applications, Springer, January 22, 2006.

[34] https://github.com/ieee8023/covid-chestxray-dataset.

[35] T. Chen, Introduction to Boosted Trees, vol. 22, University of Washington Computer Science, October 22, 2014, p. 115.